Vol 16 No 6, June 2007
1009-1963/2007/16(06)/1689-05
Chinese Physics
© 2007 Chin. Phys. Soc.
and IOP Publishing Ltd

Controlling the focusing properties of a triangular-lattice metallic photonic-crystal slab*

Feng Shuai(冯 帅)[a)†], Wang Yi-Quan (王义全)[a)],
Li Zhi-Yuan(李志远)[b)], Cheng Bing-Ying(程丙英)[b)], and Zhang Dao-Zhong(张道中)[b)]

[a)] *Academy of Physics and Electronic Engineering, Central University for Nationalities, Beijing* 100081, *China*

[b)] *Institute of Physics, Chinese Academy of Sciences, Beijing* 100080, *China*

(Received 6 October 2006; revised manuscript received 8 November 2006)

This paper studies the focusing properties of a two-dimensional photonic crystal (PC) slab consisting of a triangular lattice of metallic cylinders immersed in a dielectric background. Through the analysis of the equifrequency-surface contours and the field patterns of a point source placed in the vicinity of the PC slab, it finds that both the image distance and image quality can be controlled by simply adjusting the refractive index of the background material.

Keywords: negative refraction, photonic crystal
PACC: 4270Q, 7820P

1. Introduction

During the past few years, a novel class of media known as negative refractive-index material (NIM) has attracted a great deal of interest.[1−5] Negative refraction of electromagnetic (EM) waves is the foundation for a variety of novel phenomena and potential applications. Pendry predicted that a NIM slab could make a superlens with a resolution far beyond the diffraction limit that is inherent in the conventional far-field lens.[1]

It was shown that negative refraction can also occur in photonic crystals (PCs), which are inhomogeneous periodic array of dielectric or metallic building blocks with a lattice constant comparable to the wavelength.[6−16] Especially, Luo *et al* showed that all-angle negative refraction (AANR) could be achieved at the lowest band of two-dimensional (2D) square-lattice PCs and at a wavelength four times larger than the lattice constant.[6,7] Li and Lin showed that in addition to the negative refraction effect, other physical mechanisms such as the self-collimation effect and near-field scattering effect may play a dominant role in formation of the near-field subwavelength image.[8] Feng *et al* showed that the shape of the image formed by a square-lattice metallic PC slab can be adjusted by changing the refractive index of the background material.[9] In contrast to the images formed in the near-field region for the lowest band of a PC slab, Zhang showed that non-near-field images can be achieved in the second band of the PC slab consisting of a triangular lattice of coated cylinder in air.[10] In this paper, we will show that both the image distance and the image quality can be controlled at the second band of a PC slab consisting of a triangular lattice of metallic rods immersed in a dielectric background by simply adjusting the refractive index of the background material.

2. Simulation and discussion

A 2D triangular lattice of metallic cylinders immersed in a dielectric background with the lattice constant a is taken into consideration. The PC slab is placed in the air environment. The metallic cylinders are assumed to be perfectly conducting, so the electric field within the metal material and tangential to the metal surface is equal to zero. It turns out that metallic PCs with different dielectric backgrounds have the same band structures and equifrequency-surface (EFS) contours when they are measured with respect to the normalized frequency $n\omega$. Here, n is the refractive index of the background material, and ω is

*Project supported by the National Key Basic Research Special Foundation of China (Grant Nos 2004CB719804 and 2001CB610402), the National Natural Science Foundation of China (Grant Nos 10404036 and 10674185). The Support from the Supercomputing Center, CNIC, CAS is Also Acknowledged.
†E-mail: fengshuai75@163.com

the angular frequency of the EM wave. In this paper, the TM polarization is considered, where the electric field E_z is kept parallel to the extension axis of the metallic rods (assumed to be the z axis). In all of the simulations throughout this paper, the radius of the metallic cylinders remains $r = 0.2a$.

We employ the finite-difference time-domain (FDTD) method to calculate the band structures and EFS contours in the reciprocal space and to perform numerical simulations for the wave propagating in the finite real space.[17,18] The calculated band structures for the several lowest photonic bands along the high-symmetric lines in the first Brillouin zone are shown in Fig.1(a). It can be seen from Fig.1(a) that the metallic rods lift the first TM-polarized band and cause a stop band at the lowest frequencies. The cutoff normalized frequency of this metallic PC is $n\omega = 0.621$ (in unit of $2\pi c/a$). The second band spans from 0.812 to 1.168.

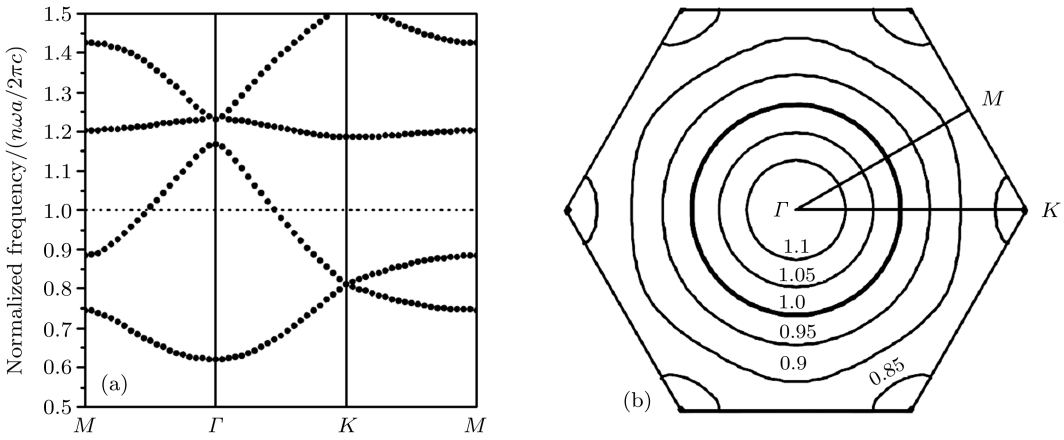


Fig.1. (a) TM-polarized photonic band structures and (b) EFS contours in the second band of the metallic PC with respect to the normalized frequency $n\omega$. The PC is composed of a triangular lattice of metallic rods in a dielectric background. The radius of the rods is $r = 0.2a$.

Figure 1(b) shows the several calculated EFS contours in the second band. It can be seen that some EFS contours such as 0.95, 1.0, and 1.1 are very close to a perfect circle, indicating that the PC can be regarded as an effective homogeneous medium at these normalized frequencies. These frequencies increase inwards. As a result, the group velocities are opposite to the phase velocities, which means that the transmitting features of the EM wave in the PC are the negative refraction behaviour. Now we visualize the propagation of EM waves through this kind of metallic PC slab by employing the FDTD method with a boundary treatment of perfectly matched layers. The rectangular metallic PC slab considered is 121 layers wide and 15 layers thick, and the surface normal is along the ΓK direction. The whole PC slab is embedded in the air environment with the refractive index equal to 1. The distances from the four slab edges to the centre of the adjacent metallic rods are $0.3a$. Thus the exact thickness of the PC slab is $12.7a$. The centre of the metallic rods in the first layer is located at $x = 0$, and the slab is symmetric with respect to $y = 0$.

A point source of continuous wave resonating at the normalized frequency $n\omega = 1.0$ is placed at the left side of the PC slab and fixed at $x = -10a, y = 0$. When the refractive indices of the background material are 2.0, 2.4, 2.7, and 3.0, the calculated E_z field patterns are shown in Figs.2(a)–(d), respectively. When the refractive index n is equal to 2.0, the frequency of the incident EM wave becomes 0.5. It can be seen from Fig.2(a) that the EM wave emitted from the point source transmits through the PC slab and travels forward, and no apparent image is formed in the opposite side of the PC slab. The EM wave front after transmitting through the PC slab first narrows, then reaches a minimum, and finally disperses into the free space. It means that negative refraction occurs under this condition and the incident EM wave is actually focused to a certain degree. The possible reason why a clearly visible image cannot be formed in the right side of the PC slab is that this frequency is much above the AANR region. A part of the incident wave with a larger incident angle cannot transmit through the PC slab in the direction of negative refraction, so no apparent image spot appears.

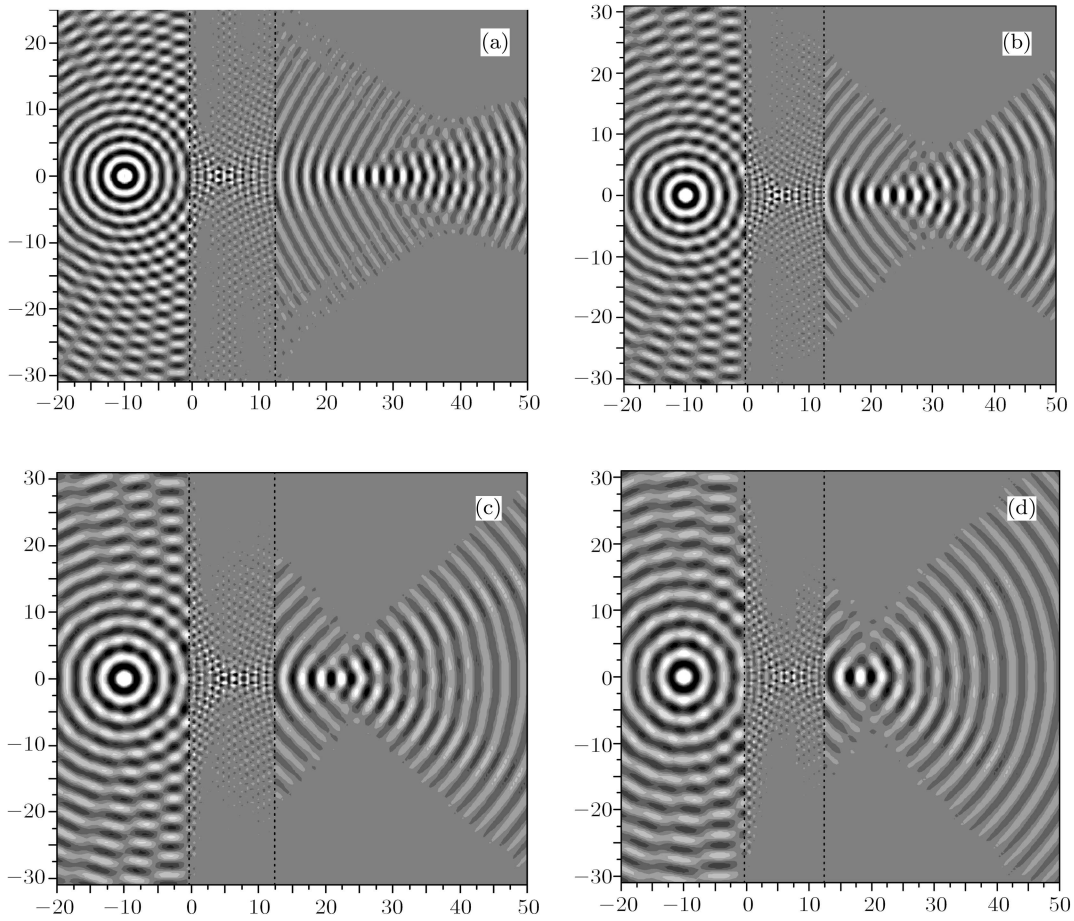


Fig.2. Simulated field distributions of a point source and its image across a metallic PC slab. The rectangular PC slab is 121 layers wide and 15 layers thick. The slab surface normal is along the ΓK direction. The distances from the left and right slab edges to the centre of the adjacent rods are all $0.3a$. The point source is placed at $x = -10a, y = 0$. The slab surfaces are represented by two dashed lines. The refractive indices of the background material are 2.0 (a), 2.4 (b), 2.7 (c), and 3.0 (d) respectively. Dark and bright regions correspond to negative and positive E_z respectively.

In order to get a visible image spot, one method we adopt is to raise the refractive index of the background material. Now we raise the dielectric refractive index to 2.4, and the corresponding frequency becomes $1.0/2.4 \approx 0.4167$ for the same normalized frequency. Figure 2(b) shows that no apparent image spot is formed in the opposite side of the PC slab. Compared with Fig.2(a), this PC slab focuses the incident EM wave to a larger degree. By increasing the refractive index of the background material, we can improve the focusing capability of the PC slab.

When the dielectric refractive index is raised to 2.7, the frequency of the incident EM wave becomes about 0.3704. As shown in Fig.2(c), a visible image is formed in right side of the PC slab. This image is a little elongated in the lateral direction and contracted in the longitudinal direction. The image spot is located at a distance $8.4a$ from the right surface of the slab. The width of the image spot is about $1.7a$, corresponding to 0.6296λ. When the refractive index n is further raised and is equal to 3.0, the corresponding excitation frequency becomes about 0.3333. Figure 2(d) shows that a good-quality image spot is formed in the right side of the PC slab. The image spot is located at a distance $5.8a$ from the right surface of the slab. The width of the image spot is about $1.6a$, corresponding to 0.5333λ.

The focusing of the EM wave within the PC slab can be clearly observed from Fig.2. With the increasing of the refractive index of the background material, the corresponding excitation frequency reduces, and the location of the focusing within the PC slab departs from the left edge and moves to the right side of the slab, which means that the effective negative refractive index of the PC slab becomes smaller and smaller. For the same normalized frequency, the ef-

fective negative refractive index of the PC slab can be controlled.

Keeping other parameters unchanged, we change the location of the point source to $x = -5$ and $y = 0$. The refractive indices of the background material are set to 3.0, 3.4, 3.74, and 4.24 in Figs.3(a), 3(b), 3(c), and 3(d) respectively. Figure 3(a) shows that a good-quality image appears in the right side of the PC slab. The centre of this image spot is located at a distance $10.8a$ from the right surface of the slab. The size of this image in the lateral direction is also about $1.6a$. Comparing Fig.2(d) with Fig.3(a), we find that the distances from the point source to the image spot are almost equal in the two situations.

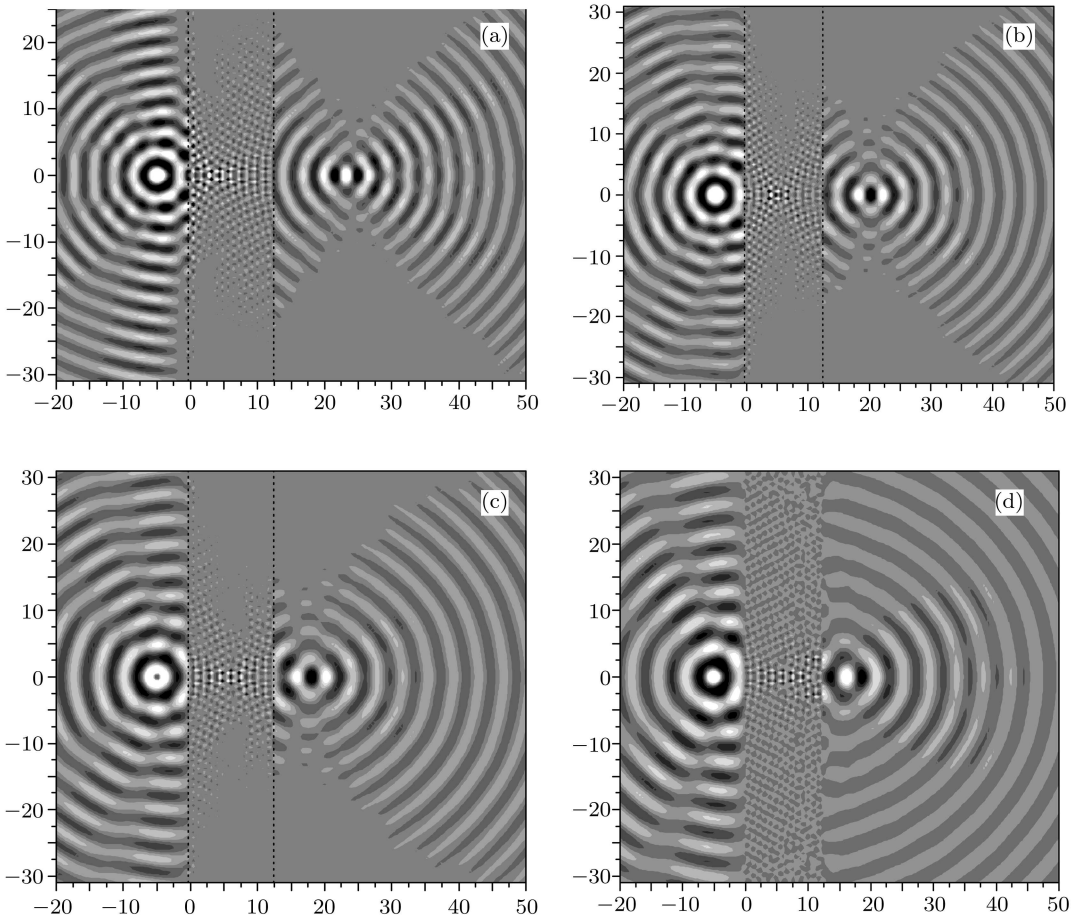


Fig.3. The same as Fig.2, but the point source is placed at $x = -5a$, $y = 0$. The refractive indices of the background material are changed to 3.0 (a), 3.4 (b), 3.74 (c), and 4.24 (d), respectively.

In the case that the refractive index of the background is changed to 3.4, an excellent-quality image appears in the right side of the PC slab, as seen from Fig.3(b). This image spot is located at a distance $7.8a$ from the right surface of the slab. The size of the image in the lateral direction is about $1.7a$, corresponding to 0.5λ. Under this condition, the distance from the point source to the centre of the image spot is twice the thickness of the PC slab. The effective refractive index of the PC slab is equal to -1 for this frequency.

If the dielectric refractive index further increases to 3.74, the corresponding incident frequency becomes about 0.2674. Figure 3(c) shows that an excellent-quality image spot also appears in the right side of the PC slab. The centre of this image spot is located at a distance $5.6a$ from the right surface of the slab. The size of the image in the lateral direction is also about $1.8a$, corresponding to 0.4813λ. Finally, the corresponding frequency becomes about 0.2358 when the dielectric refractive index n is set to 4.24. The calculated field pattern is shown in Fig.3(d). An excellent-quality image appears in the right side of the PC slab. The centre of this image spot is located at a distance $3.6a$ from the right surface of the slab. The size of the image in the lateral direction is about $1.9a$, corre-

sponding to 0.4481λ.

Comparing Figs.3(a), 3(b), and 3(c), we can see that a non-near-field image is formed in the right side of the slab, accompanied with the focusing of EM waves within the PC slab. For the same normalized frequency, the image distance shortens with the increasing of the dielectric refractive index, which means that the effective negative refractive index of the PC slab becomes smaller. As can be seen from Fig.3(d), no apparent focusing exists within the PC slab, and a bright channel connects the point source and the image spot. The width of this channel narrows, which indicates that negative refraction occurs in this case. The reason is that the effective refractive index of the PC slab for this incident frequency is much lower than -1. Therefore, the thickness of the PC slab is not thick enough to enable the focusing within itself for the certain object distance. Even under this condition, an excellent-quality image spot is also observed in the right side of the PC slab.

3. Conclusion

In summary, we have investigated the focusing properties of EM waves by 2D PC slabs consisting of a triangular lattice of metallic cylinders immersed in different dielectric backgrounds. From the analysis of the EFS contours and the corresponding field distributions under different conditions, we find that both the image distance and the image quality can be controlled in the second band by simply adjusting the refractive index of the background material. This offers a powerful way to engineer the negative refraction and focusing properties of PC slab lens.

References

[1] Pendry J B 2000 *Phys. Rev. Lett.* **85** 3966

[2] Shelby R A, Smith D R and Schultz S 2001 *Science* **292** 77

[3] Houck A A, Brock J B and Chuang I L 2003 *Phys. Rev. Lett.* **90** 137401

[4] Smith D R and Schurig D 2003 *Phys. Rev. Lett.* **90** 077405

[5] Li J S, Zhou L, Chan C T and Sheng P 2003 *Phys. Rev. Lett.* **90** 083901

[6] Luo C Y, Johnson S G, Joannopoulos J D and Pendry J B 2002 *Phys. Rev.* B **65** 201104(R)

[7] Luo C Y, Johnson S G, Joannopoulos J D and Pendry J B 2003 *Phys. Rev.* B **68** 045115

[8] Li Z Y and Lin L L 2003 *Phys. Rev.* B **68** 245110

[9] Feng S, Li Z Y, Feng Z F, Cheng B Y and Zhang D Z 2006 *Appl. Phys. Lett.* **88** 031104

[10] Zhang X D 2004 *Phys. Rev.* B **70** 195110

[11] Zhang X D and Li L M 2005 *Appl. Phys. Lett.* **86** 121103

[12] Qiu C Y, Zhang X D and Liu Z Y 2005 *Phys. Rev.* B **71** 054302

[13] Feng S, Li Z Y, Feng Z F, Cheng B Y and Zhang D Z 2005 *Phys. Rev.* B **72** 075101

[14] Feng S, Feng Z F, Ren K, Ren C, Li Z Y, Cheng B Y and Zhang D Z 2006 *Chin. Phys.* **15** 0552

[15] Wu L, Ye Z and He S L 2003 *Chin. Phys.* **12** 0642

[16] He S L, Ruan Z C, Chen L and Shen J Q 2004 *Phys. Rev.* B **70** 115113

[17] Yee K S 1966 *IEEE Trans. Antenna Propag.* **14** 302

[18] Berenger J P 1994 *J. Comput. Phys.* **114** 185